Gradu Amaierako Lana/Trabajo Fin de Grado

Fisikako Gradua/Grado en Física

Nanoscale Nuclear Magnetic Resonance

Iñigo J. Galindo Leandro

Director:
Prof. Enrique Solano
Codirector:
Dr. Jorge Casanova

Department of Physical Chemistry
Faculty of Science and Technology
University of the Basque Country UPV/EHU

Leioa, July 2019

Contents

1 Nitrogen Vacancy Centre **7**
- 1.1 Electronic structure . . . 7
- 1.2 Properties . . . 9
  - 1.2.1 Optical properties . . . 9
  - 1.2.2 Interactions . . . 10
- 1.3 Applications . . . 10

2 Theoretical Background **13**
- 2.1 The interaction picture and the Rotating Wave Approximation . . . 13
- 2.2 External fields . . . 15
  - 2.2.1 Spin magnetic resonance . . . 15
- 2.3 Decoherence . . . 18
  - 2.3.1 Ornstein-Uhlenbeck process . . . 18
  - 2.3.2 Continuous dynamical decoupling . . . 19

3 Nanoscale NMR **25**
- 3.1 Resonance of the NV Centre . . . 25
  - 3.1.1 Analytical proof . . . 26
  - 3.1.2 Numerical simulation . . . 27
  - 3.1.3 Decoherence in the case of the NV centre . . . 28
- 3.2 Sensing of ^{13}C nucleus . . . 29
  - 3.2.1 Interaction between NV-Centre and ^{13}C nucleus . . . 30
- 3.3 Numerical simulations . . . 32
  - 3.3.1 Noiseless simulation . . . 32
  - 3.3.2 Simulation with noise . . . 33

Introduction

In recent years great advances in quantum information processing, communication and sensing among other applications of quantum technologies have been made. One of the most common platforms to implement these technologies is the Nitrogen Vacancy centre (NV centre), a lattice impurity that appears in diamond. These impurities exhibit some interesting properties that make them suitable to be applied in the field of quantum technologies.

The objective of this work is to present the main characteristics of the NV centre and explain how they can be used to perform quantum sensing. For the latter I will explain a simple quantum sensing protocol that can be implemented and I will carry out numerical simulations to show its performance and results.

In the first chapter I will explain what NV centres are and, most importantly, which are the properties that make them so interesting and suitable for the development of quantum sensing.

The second chapter will introduce the required mathematical tools to face a deeper analysis of the NV centre. That is, I will explain the most important concepts that will be used to carry out the numerical simulations.

Finally, in the third chapter, I will apply the content of the first and second chapters to perform a Nanoscale Nuclear Magnetic Resonance protocol to detect a ^{13}C nucleus controlling the spin state of the NV centre. With that objective, I perform numerical simulations with MATLAB and present the results.

Chapter 1

Nitrogen Vacancy Centre

Diamonds present several crystallographic defects. These may be the consequence of irregularities within the lattice or due to the substitution of carbon atoms by other elements. The latter leads to the appearance of the so called colour centres. This kind of impurities absorb visible, infrared or ultraviolet light and give a characteristic colour to the solid[**1**].

Some of the most typical colour centres of diamond are Boron Vacancy centres (BV centres), Silicon Vacancy centres (SiV centres) , Nickel Vacancy centres (NiV centre) or Nitrogen Vacancy centres (NV centres). On this chapter we describe the NV centres. We concretely analyse their electronic structure as well as some of some of its most useful properties. Finally we explore some of the applications these impurities have. Among these we will especially focus on those related with Nanoscale Nuclear Magnetic Resonance (NNMR).

1.1 Electronic structure

NV centres along with other colour centres (BV centres, NiV centres...) are one of the many impurities that can be found in diamond structure. In particular, the NV centre is the result of the binding between a nitrogen atom and a vacancy in the crystal structure. NV centres can be created during the synthesis of the diamond itself or the diamond can be irradiated, with nitrogen ions, in order to generate vacancies within the crystal structure [**2**]. Varying the energy of this beam would lead to a change in the depth of the implant.[**2**]

As we can see in **Fig. 1.1** the nitrogen[1] atom is bonded to three neighbouring carbon atoms and to the vacancy. The nitrogen has 5 valence electrons. Three of

[1]To perform NNMR we need to apply an external static magnetic field that lifts the degeneracy of NV centre's electronic levels. Nevertheless this field also affects the nuclear states. For this reason, the NV centres that are normally used have ^{15}N. Their nuclear spin is S = 1, namely, it is a three level system with $|-1\rangle_{\mathrm{N}}$, $|1\rangle_{\mathrm{N}}$ and $|0\rangle_{\mathrm{N}}$ states. We could then polarise the nucleus in the $|0\rangle_{\mathrm{N}}$ state and thus the structure of the NV centre would remain unaltered.

If the nitrogen atom was ^{14}N the nuclear spin would be S = 1/2 and its state would affect the structure of the NV centre.

(a) (b)

Figure 1.1: Primitive cells of diamond (a) and diamond with a NV centre (b). Grey represents carbon atoms, blue represents nitrogen and white a vacancy. The side of the primitive cell is about 0.35 nm long.

them form a covalent bond with the electrons of the surrounding carbon atoms and the remaining two stay a lone pair. The vacancy, on the other side, has 4 electrons. Three of them come from the surrounding carbon atoms and the forth one is taken from the lattice. Two of these electrons on the vacancy form a bond. Thus we get two free electrons in the vacancy that form a system with spin S = 1. This charge state is known as NV^-. This is the charge state we are interested in. [**3**][2].

As stated above, there are two free electrons in the NV centre and this generates a system with spin S = 1. Consequently a triplet ground level $^3A_2$ and a triplet excited level ^3E appear [**3**]. These two levels have a spin conserving optical transition with $\lambda = 637$ nm. There are also another two metastable singlet levels $^1A_1$ and ^1E [**3**].

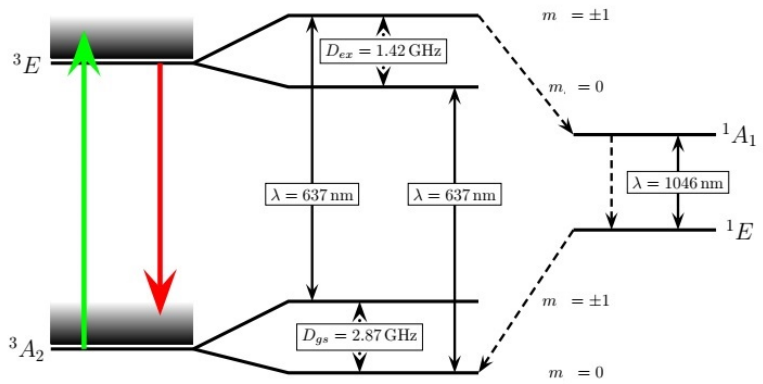

Figure 1.2: Energy levels of NV^-. Continuous lines indicate radiating transitions, while dashed lines indicate non radiating transition. Image taken from [**2**].

The spin Hamiltonian of the NV centre is[3] [**2**]

[2]There is also another relevant charge state of the NV centre (NV^0) which only has one free electron in the vacancy. Theoretically this charge state of the NV centre should have two hyperfine states with $m = \pm 1/2$. This would allow to perform NNMR, but these states have not been experimentally observed [**3**]. Thus it is impossible to use NV^0 to perform NNMR and we are not interested in it.

[3]In this work we adopt the convention $\hbar = 1$

$$H = D_{gs}\left(\mathrm{S}_z^2 - \frac{1}{3}[\mathrm{S}(\mathrm{S}+1)]\right) + \vec{\mathrm{S}}\mathbf{A}_N\vec{\mathrm{I}}_N + \sum_i(\vec{\mathrm{S}}\mathbf{A}_i\vec{\mathrm{I}}_i) \tag{1.1}$$

with $D_{gs} = (2\pi)\times 2.87$ GHz[**2**] and S_z is the electronic z-spin operator. This is the ground state zero field splitting, namely the splitting between $m = 0$ and $m = \pm 1$ states. The z-axis is chosen to be the symmetry axis of the NV centre, that is, the axis that is parallel to the line connecting the nitrogen atom and the vacancy in **Fig. 1.1**.

The second term in the Hamiltonian represents the hyperfine interaction of the NV centre's nitrogen atom. $\vec{\mathrm{S}}$ is the electronic spin operator, $\mathbf{A}_N$ is the hyperfine interaction tensor and $\vec{\mathrm{I}}_N$ is the operator of nitrogen's nuclear spin. The last term in **Eq. (1.1)** represents the interaction of the NV centre with its surrounding spin bath. However, this form of the Hamiltonian is not used throughout this project. To carry out the simulations we will simply take the first term with $\mathrm{S} = 1$ and substitute the latter terms with a stochastic function that will simulate their effect

$$H = D_{gs}\left(\mathrm{S}_z^2 - \frac{2}{3}\right) + \frac{\delta(t)}{2}\mathrm{S}_z. \tag{1.2}$$

Where the added term represents the stochastic function mentioned above.

The term $-2/3$ does not contribute to the analysis and numerical simulations in this work so we can ignore it. Finally the Hamiltonian we consider for the electronic ground state is:

$$H = D_{gs}\left(\mathrm{S}_z^2\right) + \frac{\delta(t)}{2}\mathrm{S}_z \tag{1.3}$$

1.2 Properties

1.2.1 Optical properties

One of the most interesting kind of properties the NV centre presents are the optical ones since they allow us to readout its spin state and polarize it.

If we illuminate the impurity with visible radiation (typically 532 nm), the NV centre emits radiation. During approximately the first 300 ns of illumination get a contrast between the luminosity of both radiative decays (continuous lines in **Fig. 1.2**)[**4**]. This is because the excited state with $m = \pm 1$ has a non radiative decay path through the singlet levels to the ground state level with $m = 0$. This contrast allows to read out the spin state of the NV centre.

After the illumination the system will be partly polarised in the $|\,^3A_2; m = 0\rangle = |0\rangle$ state and partly in the $|\,^3A_2; m = \pm 1\rangle = |\pm 1\rangle$ state [**4**]. Polarisations in the $|0\rangle$ state between 46% and 96% have been reported at room temperature [**3**], while polarisations larger than 99% haven achieved at low temperatures of ≈ 4 K [**5**].

1.2.2 Interactions

Other useful properties the NV centres exhibit are their interactions with the lattice and with external fields.

Diamond exhibits a natural abundance of a 1.1% of ^{13}C ($S_C = 1/2$). This spin bath interacts with the NV centre and it is the main source of decoherence[4]. At room temperature and with no external field acting upon the NV centre, it loses its coherence after a time $T_2^* = 10$ μs [**6**]. However, if we 'protect' the NV centre (for instance, applying an external oscillating magnetic field) we can extend this coherence time up to $T_2 = 1.8$ ms [**3**][5]. This coherence time allows the coupling between the impurity and surrounding spins to be manipulated.[**3**].

Besides these interactions with the surrounding spins the NV centre also exhibits a strong interaction with external magnetic fields which allows us to extend the coherence time as well as to lift the degeneracy of the $|\pm 1\rangle$ state. This last feature will be analysed later on and we will see how useful this property of the NV centres is.

1.3 Applications

In recent years NV Centres have emerged as entities with a great variety of applications. This is due to their high stability, their optical activity and their strong interaction with magnetic, electric and strain fields.

Some of the most important applications are nanoscale sensing, ion concentration monitoring, strain and pressure sensing, scanning magnetometry or NNMR [**7**]. In this work we focus on the last one.

One way of performing NNMR consists of putting the quantum system on a high magnetic field and measuring the Larmor precession of the surrounding nuclear spins [**7**]. In this manner, we can detect different nuclei surrounding the NV Centre. This protocol might, for example, enable us to know the internal structure of proteins and biological systems in a more precise way [**7**].

In the last chapter we simulate an experiment where the NV centre evolves under the an oscillating magnetic field. The amplitude of the field would be varied. For each amplitude we would let the system evolve a certain time and we would then check the spin state of the NV centre. Checking which value of the amplitude provokes a change in NV centre's spin state, would allow us to determine the gyromagnetic ratio of the surrounding nuclear spins. If we know the gyromagnetic ratio we can deduce what type of nuclei we detect.

Evidently, in our simulation we previously know the gyromagnetic ratio of the

[4]We refer to coherence time as the time during which some quantum mechanical properties (entanglement or superposition for instance) of the system are not affected by the environment. Decoherence is thus the loss of those quantum mechanical properties

[5]From now on we refer to the coherence time of the unprotected NV centre as T_2^*. On the other hand T_2 will be the coherence time of the protected NV centre.

element (^{13}C in our case) and such deduction will not be made. Our aim is to predict which result we could expect in such experiment.

Chapter 2

Theoretical Background

In this chapter we introduce the necessary theoretical background to make a deeper analysis of the NV centre and its applications. The following mathematical tools as well as the information exposed in the previous chapter will be applied in the third chapter to perform numerical simulations of a Nanoscale Nuclear Magnetic Resonance protocol.

2.1 The interaction picture and the Rotating Wave Approximation

There are three different pictures with which we can treat quantum mechanical systems. Typically, one considers the Schrödinger, Heisenberg and interaction pictures. We are only interested in the Schrödinger and interaction pictures.

In the Schrödinger picture we suppose that state kets

$$|\alpha\rangle \tag{2.1}$$

evolve in time affected just by the time evolution operator

$$e^{-iH_0t} \tag{2.2}$$

where H_0 is the Hamiltonian. Namely, in the Schrödinger picture we would have

$$|\alpha, t\rangle = e^{-iH_0t} |\alpha\rangle . \tag{2.3}$$

Let us now suppose we have the following Hamiltonian describing our system.

$$H = H_0 + V(t). \tag{2.4}$$

Where $V(t)$ is a time dependent potential.

We now define the quantum state of a system in the interaction picture as [**8**]

$$|\alpha, t\rangle_I = e^{iH_0 t} |\alpha, t\rangle . \tag{2.5}$$

Where the ket at the right hand side is the quantum state in the Schrödinger picture.

The operators in the interaction picture are

$$A_I = e^{iH_0 t} A e^{-iH_0 t}. \tag{2.6}$$

The potential of the Hamiltonian **Eq.** (**2.4**) in the interaction picture is thus

$$V_I = e^{iH_0 t} V(t) e^{-iH_0 t}. \tag{2.7}$$

If we now take the time derivative of **Eq.** (**2.5**) and consider the Hamiltonian of the system to be **Eq.** (**2.4**) we get the following,

$$\begin{aligned} i\frac{\partial}{\partial t} |\alpha, t\rangle_I =& i\frac{\partial}{\partial t} \left(e^{iH_0 t} |\alpha, t\rangle\right) && (2.8)\\ &= -H_0 e^{iH_0 t} |\alpha, t\rangle + e^{iH_0 t}(H_0 + V(t)) |\alpha, t\rangle && (2.9)\\ &= e^{iH_0 t} V e^{-iH_0 t} e^{iH_0 t} |\alpha, t\rangle . && (2.10) \end{aligned}$$

Then, we find an equation similar to Schrödinger's:

$$i\frac{\partial}{\partial t} |\alpha, t\rangle_I = V_I |\alpha, t\rangle_I . \tag{2.11}$$

That is why we refer to V_I as the interaction Hamiltonian. We can use V_I to know the evolution of the system in the same way we use the Hamiltonian in the Schrödinger picture.

When defining the potential in the interaction picture **Eq.** (**2.7**) we might get some terms within it that rotate much faster than others. If this were the case we could apply the RWA (Rotanting Wave Approximation), that is, we could ignore those terms since they would hardly contribute to the evolution of the system. This can be better visualised with the following example. Let us suppose we have the following Hamiltonian of a system with S=1/2,

$$H = E_0 \sigma_z + \Omega \sigma_x cos(\omega t) = E_0 \sigma_z + \frac{\Omega \sigma_x}{2} \left(e^{i\omega t} + e^{-i\omega t}\right) . \tag{2.12}$$

Where σ matrices are Pauli matrices and we take $|\uparrow\rangle$ (m=1/2) and $|\downarrow\rangle$ (m=-1/2) as our base.

We now take the interaction picture with respect to $E_0\sigma_z$ and we get

$$H_I = \frac{\Omega}{2}\left(e^{i\omega t} + e^{-i\omega t}\right)\left(|\downarrow\rangle\langle\uparrow| e^{-iE_0 t} + |\uparrow\rangle\langle\downarrow| e^{iE_0 t}\right). \tag{2.13}$$

The exponentials with $\omega + E_0$ rotate much faster than the other ones, thus we can ignore them. We get

$$H_I = \frac{\Omega}{2}\left(|\downarrow\rangle\langle\uparrow| e^{-it(E_0-\omega)} + |\uparrow\rangle\langle\downarrow| e^{it(E_0-\omega)}\right) \tag{2.14}$$

Both the interaction picture and the RWA are widely used throughout this work to reach some interesting results and to ease computation.

2.2 External fields

We now study the evolution of the NV centre subject to both static and oscillating external magnetic fields.

2.2.1 Spin magnetic resonance

Perturbation through a static magnetic field

If we apply an external static magnetic field, $\vec{B} = B_z\hat{z}$, we add the following term

$$\Delta H = -\vec{\mu}\cdot\vec{B} \tag{2.15}$$

where $\vec{\mu} = \gamma_e\vec{\mathrm{S}}$ and where $\gamma_e = 2\pi \times 28$ GHz/T[**7**] is the gyromagnetic ratio.

As it has been pointed out, we only have magnetic field in the z-axis direction. This means

$$\Delta H = -\gamma_e \mathrm{S}_z B_z \tag{2.16}$$

The eigenvalues of this term are

$$\Delta E = -\gamma_e B_z m \tag{2.17}$$

where $m = \pm 1, 0$. $\gamma_e B_z$ is called the Larmor frequency.

Rabi cycle

If we apply an external static magnetic field in the z-axis to the NV centre the degeneracy will be lifted in the $|^3A_2; m = \pm 1\rangle$ level. But for the analysis of the Rabi cycle we treat the problem as a two level problem. The levels are labelled as $|0\rangle = |^3A_2; m = 0\rangle$ and $|1\rangle = |^3A_2; m = \pm 1\rangle$. We call them ground and excited states respectively.

The hamiltonian in the Schrödinger picture of a two level system subject to a weak magnetic field is

$$H = \omega \left|1\right\rangle \left\langle 1\right| - \vec{\mu} \cdot \vec{B} \tag{2.18}$$

With ω being the frequency between both ground and excited states.

$\vec{\mu} = \gamma_e \vec{\sigma}$ is the magnetic dipole moment operator.

The magnetic field is an oscillating one

$$\vec{B} = \frac{\vec{B_0}}{2}\left(e^{i\omega_L t} + e^{-i\omega_L t}\right)$$

So the time dependent part of the Hamiltonian is

$$H'(t) = \gamma_e \vec{\sigma} \cdot \frac{\vec{B_0}}{2}\left(e^{i\omega_L t} + e^{-i\omega_L t}\right) \tag{2.19}$$

Taking $\vec{B_0} = B_0 \hat{x}$, we would get the following in the interaction picture with respect to $\omega \left|1\right\rangle \left\langle 1\right|$:

$$H'_I(t) = \frac{\gamma_e B_0}{2}\left(\left|1\right\rangle \left\langle 0\right| \left(e^{i(\omega+\omega_L)t} + e^{i(\omega-\omega_L)t}\right) + \left|0\right\rangle \left\langle 1\right| \left(e^{i(-\omega+\omega_L)t} + e^{-i(\omega+\omega_L)t}\right)\right) \tag{2.20}$$

We can ignore the exponentials with $\omega + \omega_L$ because they rotate a much faster rate than the frequency $\omega - \omega_L$. We get the following interaction Hamiltonian

$$H'_I(t) = \frac{\gamma_e B_0}{2}\left(\left|1\right\rangle \left\langle 0\right| \left(e^{i(\omega-\omega_L)t}\right) + \left|0\right\rangle \left\langle 1\right| \left(e^{-i(\omega-\omega_L)t}\right)\right) \tag{2.21}$$

This indicates that the oscillating magnetic field provokes the system to transition between two levels. We get a better perspective of this turning back to the Schrödinger picture and solving the system.

We first introduce the Hamiltonian H in the time dependent Schrödinger equation

$$i\hbar \frac{\partial}{\partial t} \left|\psi\right\rangle_S = H \left|\psi\right\rangle_S \tag{2.22}$$

and considering that the state of the system is $\left|\psi\right\rangle_S = c_0 \left|0\right\rangle + c_1 \left|1\right\rangle$[1], the following system of equations is obtained

[1] S subscript indicates that we are working in the Schrödinger picture

$$i\frac{dc_0}{dt} = \frac{\gamma_e B_0}{2} e^{i\omega_L t} c_1 \tag{2.23}$$

$$i\frac{dc_1}{dt} = \omega c_1 + \frac{\gamma_e B_0}{2} e^{-i\omega_L t} c_0. \tag{2.24}$$

Now, we change to the interaction picture

$$|\psi\rangle_I = \alpha\,|0\rangle + \beta\,|1\rangle = e^{iH_0 t}\,|\psi\rangle_S = e^{i|1\rangle\langle 1|\omega t}\,|\psi\rangle_S \tag{2.25}$$

Where $H_0 = \omega\,|1\rangle\langle 1|$. Now we apply the $e^{i|1\rangle\langle 1|\omega t} = \sum_0^\infty \frac{(i\omega t\,|1\rangle\langle 1|)^n}{n!}$ operator in each component of $|\psi\rangle_S$ and we get

$$|\psi\rangle_I = \alpha\,|0\rangle + \beta\,|1\rangle = c_0\,|0\rangle + c_1 e^{i\omega t}\,|1\rangle \tag{2.26}$$

This means that

$$\alpha = c_0 \tag{2.27}$$

$$\beta = c_1 e^{i\omega t} \tag{2.28}$$

We define how far the frequency of the applied field is from resonance as $\delta = \omega_L - \omega$. We call this quantity the detuning.

Finally we get this set of equations

$$\frac{d\alpha}{dt} = \frac{\gamma_e B_0}{2} e^{i\delta t}\beta \tag{2.29}$$

$$\frac{d\beta}{dt} = \frac{\gamma_e B_0}{2} e^{-i\delta t}\alpha \tag{2.30}$$

We call $\gamma_e B_0 = \Omega$.

Solving these equations leads to

$$|\alpha(t)|^2 = \frac{\Omega^2}{(\Omega/2)^2 + (\delta/2)^2} \sin^2\left(\sqrt{(\Omega/2)^2 + (\delta/2)^2}\,t\right). \tag{2.31}$$

This is the probability of finding the system in the fundamental level $|0\rangle$ after a time t.

The analysis above implies, as we mentioned at the beginning of this section, that when we apply an external oscillating magnetic field to a two level system, it starts flipping between both levels and thus the spin state of the system changes. This

result will be of great help later on. We will concretely see that, in fact, the Rabi cycle, and therefore the change in the spin state, will only happen under certain conditions. Observing the change in the spin state and knowing in advance these conditions is what allows us to perform the quantum sensing protocol in the third chapter.

2.3 Decoherence

As explained on the first chapter the NV centre can get a long coherence time at room temperatures. On this section we explain how we are going to model the main source of decoherence and we present a way of extending this coherence time.

2.3.1 Ornstein-Uhlenbeck process

In the first chapter we presented the complete Hamiltonian of the electronic ground state of the NV Centre in **Eq.** (**1.1**). The main source of decoherence on the NV centres is the spin bath of ^{13}C [**3**]. To represent the effect of the spin bath upon the NV Centre we use, as mentioned, a stochastic function. This stochastic function is in our case described by an Ornstein-Uhlenbeck (OU process). The function has this form:

$$\delta(t+\Delta t) = \delta(t)e^{-\Delta t/\tau} + \left[\frac{c\tau}{2}\left(1-e^{-2\Delta t/\tau}\right)\right]^{1/2} N(t) \tag{2.32}$$

Where $N(t)$ refers to a temporally uncorrelated random variable that ranges between 0 and 1, c is the diffusion constant that depends only on τ (correlation time) and T_2^* (coherence time) [**9**]. The explicit form of c is:

$$c = \frac{4e^{2T_2^*/\tau}}{\tau^2(4e^{T_2^*/\tau}\tau - \tau + e^{2T_2^*/\tau}(2T_2^* - 3\tau))} \tag{2.33}$$

The function looks like this

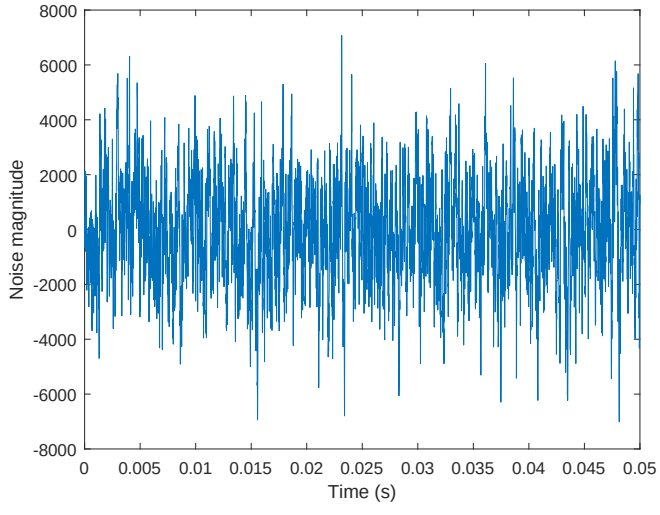

Figure 2.1: Plot a an OU process. This plot was drawn with variables $\tau = 5 \cdot 10^{-5}$ s, $\Delta t = 10^{-5}$ s and $c = 1.5 \cdot 10^{11}$.

We could really use any stochastic function to simulate the effect of the spin bath on the NV centre, but there are two main reasons to use the Ornstein-Uhlenbeck process.

On the one hand, this process simulates a noise that is not white, namely it is centred around some frequencies[**9**]. This way we are able to depict a more realistic scenario when simulating.

On the other hand, we saw above that the Ornstein-Uhlenbeck process only depends of T_2^* and τ. These are both values that can be experimentally measured. We can take advantage of that to simulate the actual effect of the surroundings in a very accurate way. In the simulations we concretely use $T_2^* = 10$ μs and $\tau = 1$ ms. These are experimental values obtained through a private communication with Prof. Boris Naydenov (Ulm University, Germany).

2.3.2 Continuous dynamical decoupling

One of the greatest problems one is faced with when treating with quantum mechanical systems, such as NV centres, is the coherence time. As we mentioned, this is the time some properties of quantum mechanical system such as superposition or entanglement do not get affected by the environment. The two level system described above has its own specific coherence time. It is of critical importance to be able to extend this coherence time so we can take advantage of the useful properties quantum mechanical systems exhibit.

Now we talk about the continuous dynamical decoupling, a method one can extend the coherence time with.

Let us suppose that the Hamiltonian of a system with spin S = 1/2 is

$$H = \frac{\gamma B_0}{2}\sigma_z = \frac{\omega_0}{2}\sigma_z. \tag{2.34}$$

To reflect the effect of the environment we introduce a new time dependent term in out Hamiltonian.

$$H = \frac{\omega_0}{2}\sigma_z + \frac{\delta(t)}{2}\sigma_z \tag{2.35}$$

This new term reflects the noise we would have in our experiment. The function $\delta(t)$ represents a stochastic process. In this case an Orstein-Uhlenbeck process has been chosen.

If we now represent our Hamiltonian in the interaction picture with respect to $\frac{\omega_0}{2}\sigma_z$ we get

$$H_I = \frac{\delta(t)}{2}\sigma_z \tag{2.36}$$

Because the Hamiltonians at different times commute, the time evolution operator of the system would then be given by

$$U(t, t_0) = \exp\left[-i\int_{t_0}^{t}\frac{\delta(t')\sigma_z}{2}dt'\right] \tag{2.37}$$

If we choose our time interval ($\Delta t = t - t_0$) to be very small with respect to the correlation time we can approximate this operator in the interval Δt to

$$U(t, t_0) \approx \exp\left[-i\delta(t)\sigma_z\Delta t\right] \tag{2.38}$$

With this approximation we can simulate how a system whose initial state is $|\uparrow\rangle_x = \frac{1}{\sqrt{2}}(|\downarrow\rangle + |\uparrow\rangle)$ evolves through time. The evolution is reflected in te following plots.

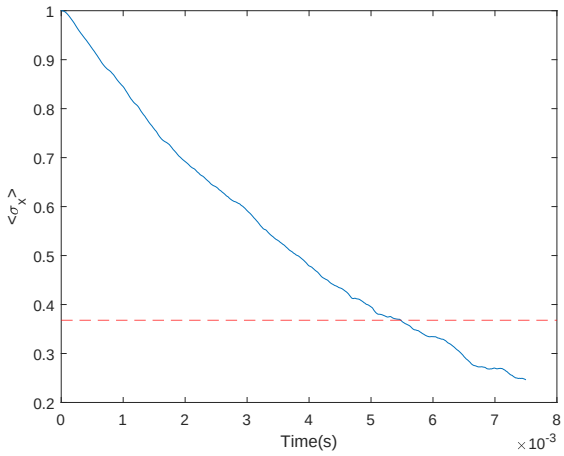

Figure 2.2: $\langle \sigma_x \rangle$ with respect to time (seconds). For this simulation we took the following numerical values $\tau = 50\mu s$, $c = 1.5 \cdot 10^{11}$ and $\Delta t = 0.5\mu s$. We did 1000 shots and averaged them. The dashed red line indicates the coherence time. We needed 511.166 s to compute this.

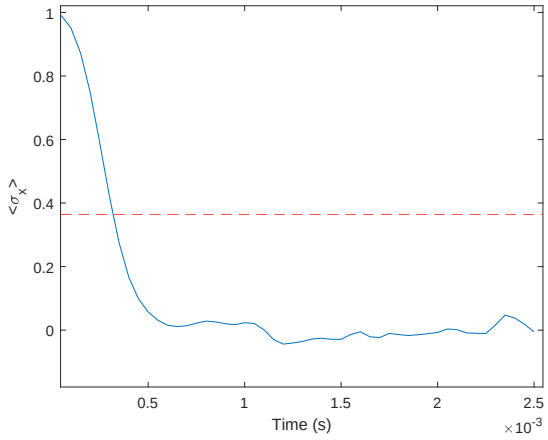

Figure 2.3: $\langle \sigma_x \rangle$ with respect to time (seconds). For this simulation we took the following numerical values $\tau = 5ms$, $c = 1.5 \cdot 10^{11}$ and $\Delta t = 0.05ms$. We did 1000 shots and averaged them. The dashed red line indicates the coherence time. We needed 2.395 s to simulate this.

These plots show the different kind of decays that can be simulated with the OU process. On the one hand the exponential decay represented by **Fig. 2.2** and the Gaussian decay **Fig. 2.3**. This decays appear depending on the relation between T_2^* and τ. If $T_2^* << \tau$ the decay is Gaussian and if $T_2^* \approx \tau$ the decay is exponential [**9**]. In the case of the NV centre we later see that the decay is Gaussian.

In both plots we can now identify the coherence time. This corresponds to the time in which the system decays $1/e$ of its initial value.

Our aim is now to extend the coherence time. In order to do that we introduce a driving field. In the interaction picture with respect to $\frac{\omega_0}{2}\sigma_z$ the Hamiltonian of the system is

$$H_I = \frac{\delta(t)}{2}\sigma_z + \Omega\cos(\omega t)\sigma_x. \tag{2.39}$$

Following a similar procedure as when solving the Rabi cycle and making the the Rotating Wave Approximation we get to

$$H_I = \frac{\delta(t)}{2}\sigma_z + \frac{\Omega}{2}\sigma_x \tag{2.40}$$

In the following graphs we see the evolution of the system that undergoes due to Hamiltonians (**2.39**) and (**2.40**) if we start in the $|+\rangle_x$ apply the time evolution operator $U(t, t_0) = e^{iH\Delta t}$ several times.

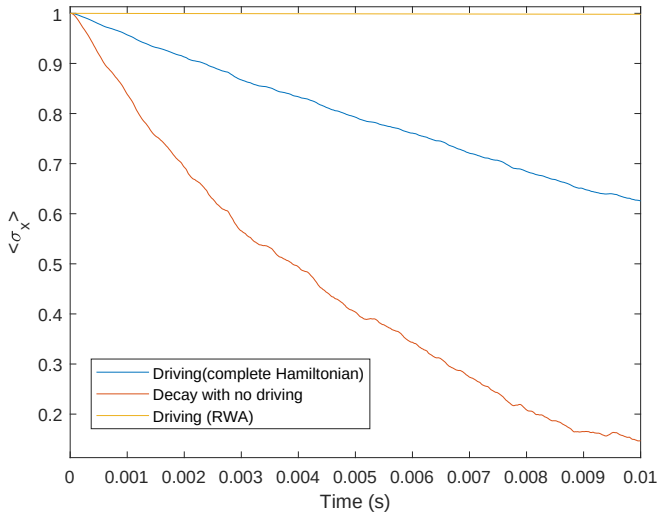

Figure 2.4: $\langle\sigma_x\rangle$ with respect to time. $\tau = 50\mu s$, $\Delta t = 0.5\mu s$, $c = 1.5 \cdot 10^{11}$ and $\Omega = 2\pi \cdot 0.5$KHz. In the case of the complete Hamiltonian, namely, the one with the $\Omega\cos\omega t$ term, $\omega = 2\pi \cdot 1$MHz has been used. We averaged 750 shots. We used 3792.672 s to perform this simulation.

We should also take into account that if the amplitude of the driving (the Ω frequency) lies in the region where the noise spectrum is negligible, the effect of the stochastic function can also be neglected. In the graph below we can appreciate how the coherence time grows as we increase Ω.

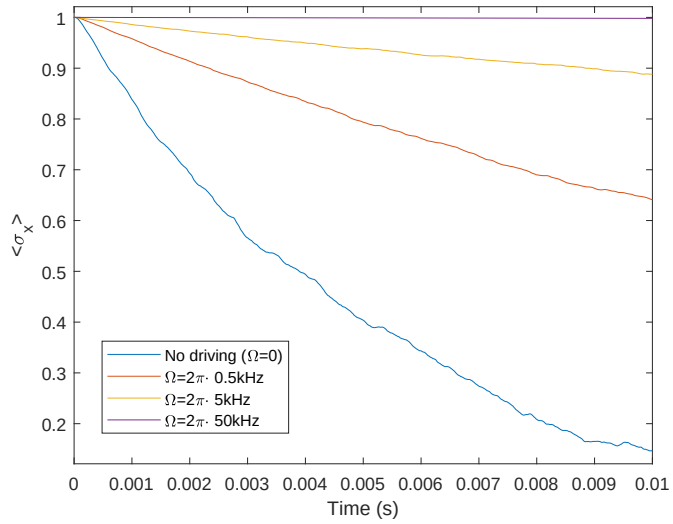

Figure 2.5: $\langle \sigma_x \rangle$ with respect to time for different Ω frequencies. Same numerical values as in the prior simulation were used, but changing Ω from case to case. We averaged 750 shots. We needed 5080.870 s to compute the result.

If we calculated the Fourier Transform of the Ornstein-Uhlenbeck process we would see that the frequencies involved are centred around certain value. If we take the Ω frequency away from those central values the effect of the noise will be diminished since it would not interfere with the flopping. That is what the plots above reflect [**9**].

Chapter 3

Nanoscale NMR

In this final chapter we finally apply all the data presented before to the case of the NV centre and we simulate a Nanoscale Nuclear Magnetic Resonance protocol that will allow us to detect the presence of a nuclear spin in the surroundings of the impurity.

3.1 Resonance of the NV Centre

As explained before, if a two level system were put under the effect of an oscillating magnetic field, the system would transition periodically between the fundamental and the excited level. At first this might seem inapplicable to the NV centre described because it is in fact a three level system. But it can be mathematically shown that, if the NV centre is driven with an oscillating field with the appropriate frequency, the system would only be able to transition between the state $|0\rangle$ and one of the $|1\rangle$ or $|-1\rangle$ states[1]. This happens if the frequency of the oscillating field is equal to that of the splitting between $|0\rangle$and $|1\rangle$ or $|-1\rangle$, i.e., the frequency of the field must be equal to

$$\omega = D_{gs} \pm \gamma_e B_z \tag{3.1}$$

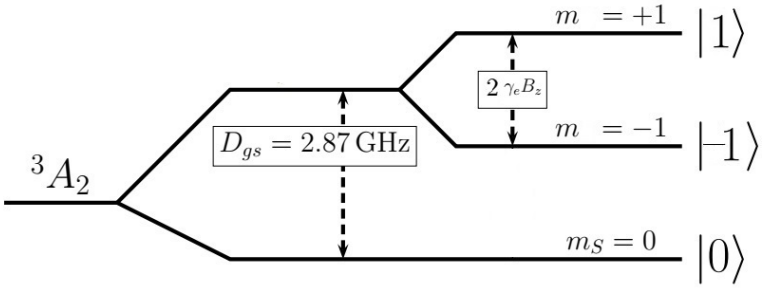

Figure 3.1: Energy levels of the ground state. The degeneracy of the $|\,^3A_2; m = \pm 1\rangle = |\pm 1\rangle$ level is lifted with the B_z field. Image taken from [**2**].

[1]The quantum numbers -1 and 1 correspond to the magnetic quantum number m.

We now show this fact both analytically and numerically.

3.1.1 Analytical proof

The Hamiltonian of a NV centre affected by a magnetic field in the z-direction is the following

$$H = D_{gs}\mathrm{S}_z^2 - \gamma_e B_z \mathrm{S}_z = (D_{gs} + |\gamma_e| B_z)\,|1\rangle\langle 1| + (D_{gs} - |\gamma_e| B_z)\,|-1\rangle\langle -1| \tag{3.2}$$

Introducing the following oscillating magnetic field

$$|\gamma_e| B_0 \mathrm{S}_x \cos\omega t = \Omega \mathrm{S}_x \cos\omega t \tag{3.3}$$

and changing to the interaction picture with respect to **Eq. (3.2)** we get

$$H_I = \frac{\Omega}{2}(|1\rangle\langle 0|\, e^{i(\omega_{10}t)} + |-1\rangle\langle 0|\, e^{i(\omega_{-10}t)} + \text{H.c.})(e^{i\omega t} + e^{-i\omega t}) \tag{3.4}$$

where $\omega_{\pm 10} = D_{gs} \pm |\gamma_e| B_z$.

Developing the expression a bit more

$$\begin{aligned} H_I = \frac{\Omega}{2}(&|1\rangle\langle 0|\, e^{i(\omega_{10}-\omega)t} + |1\rangle\langle 0|\, e^{i(\omega_{10}+\omega)t} + \\ &|-1\rangle\langle 0|\, e^{i(\omega_{-10}+\omega)t} + |-1\rangle\langle 0|\, e^{i(\omega_{-10}-\omega)t} + \text{H.c.}) \end{aligned} \tag{3.5}$$

If we now take $\omega = \omega_{10}$ and make the rotating wave approximation, i.e., we ignore all the terms much bigger or much lower than ω_{10}, we get

$$H_I = \frac{\Omega}{2}(|1\rangle\langle 0| + |0\rangle\langle 1|) = \frac{\Omega}{2}\begin{bmatrix} 0 & 0 & 0 \\ 0 & 0 & 1 \\ 0 & 1 & 0 \end{bmatrix} \tag{3.6}$$

From now on we call $\begin{bmatrix} 0 & 0 & 0 \\ 0 & 0 & 1 \\ 0 & 1 & 0 \end{bmatrix} = M$.

This means that the propagator of the Hamiltonian would be

$$U(t) = e^{\frac{-i\Omega}{2}Mt} \tag{3.7}$$

This exponential can be split in two summations of even and odd terms

$$U(t) = \sum_{n=0}^{\infty} \frac{(-i\Omega t/2)^{2n}}{(2n)!} M^{2n} + \sum_{n=0}^{\infty} \frac{(-i\Omega t/2)^{2n+1}}{(2n+1)!} M^{2n+1} \tag{3.8}$$

Using recurrence relations it can be easily shown that

$$M' = M^{2n} = \begin{bmatrix} 0 & 0 & 0 \\ 0 & 1 & 0 \\ 0 & 0 & 1 \end{bmatrix} \tag{3.9}$$

$$M^{2n+1} = \begin{bmatrix} 0 & 0 & 0 \\ 0 & 0 & 1 \\ 0 & 1 & 0 \end{bmatrix} \tag{3.10}$$

Thus,

$$U(t) = M \sin\left(\frac{\Omega t}{2}\right) + M' \cos\left(\frac{\Omega t}{2}\right) \tag{3.11}$$

If we began our experiment in the base state $|0\rangle$ and after a certain time $t = t_0$ we calculated the probability of finding our system in that same state we would find the following

$$\langle 0| U(t_0) |0\rangle = \cos\left(\frac{\Omega t_0}{2}\right) \rightarrow P(|0\rangle)_{t=t_0} = \cos^2\left(\frac{\Omega t_0}{2}\right) \tag{3.12}$$

According to the analysis we just made, we can only have transitions between the state $|0\rangle$ and $|1\rangle$ if we choose the frequency of the driving field to be ω_{10}.

In the following section we give a numerical proof that validates the conclusions reached here.

3.1.2 Numerical simulation

To make the following simulation **Eq. (2.39)** was taken to define the propagator

$$U(t, t_0) = e^{-i \int_0^{t_0} H_I(\omega, t) dt} \tag{3.13}$$

Taking sufficiently small time intervals between $t = 0$ and $t = t_0$ it is possible to approximate this propagator as

$$U(t, t_0) = \Pi_{k=0}^{n} e^{-iH_I(\omega,t)t_k - t_{k-1}} = \Pi_{k=0}^{n} e^{-iH_I(\omega,t)\Delta t} \tag{3.14}$$

Fig. 3.2 shows the probability of finding the system in the $|0\rangle$ state after a certain time t_0 with respect to different driving frequencies.

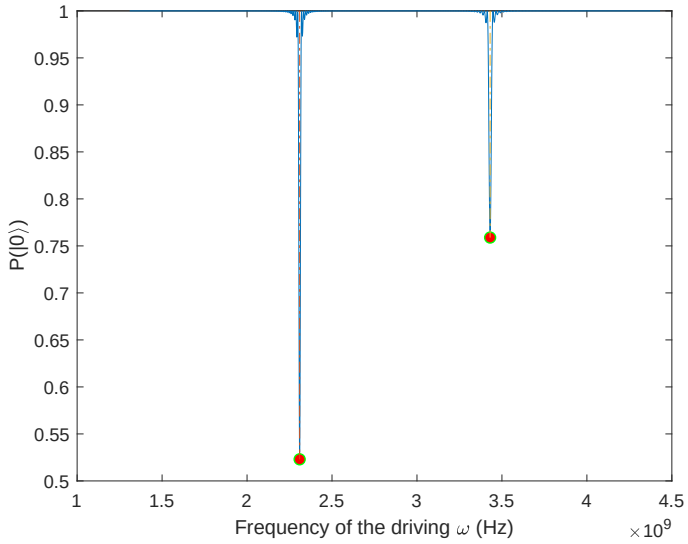

Figure 3.2: Probability of finding the system in the $|0\rangle$ state after $t = 200\frac{1}{\omega}$ with respect to ω. The numerical values that were used in the simulation were $\gamma_e = 2\pi \times 28.024 \cdot 10^9$ Hz/T, $D_{gs} = 2\pi \times 2.87 \cdot 10^9$Hz/T, $\Omega = -1.9816 \cdot 10^6$Hz and $B_z = 0.02$T. Different time intervals(Δt) were used for different driving frequencies. This simple equation was used $\Delta t = 1/(\omega \times \text{iterations})$. In the present case iterations=200. This way one single oscillation was divided in 200 steps. Since the propagator is periodical, then it was only necessary to raise it to the power of 200 so we could get the propagator that took the system from $t = 0$ to $t = 200\frac{1}{\omega}$. The dots indicate the analytical result. We needed 68.236s to simulate this.

Thus, the analytical proof gets confirmed. There are only two frequencies at which the system can jump from $|0\rangle$ to $|-1\rangle$ (first peak in the graphic, with $\omega = 2.3095 \cdot 10^9$ Hz) and to $|1\rangle$ (second peak in the graphic, with $\omega = 3.4305 \cdot 10^9$ Hz). In fact, if the probability in equation (**3.12**) is computed, we get the exact value of the peaks.

Now we can go on and start making more a more complex analysis of the system of the NV centres and its surroundings.

3.1.3 Decoherence in the case of the NV centre

Now, we must take into account that if we choose a resonant frequency as the frequency of the driving the system will only make transitions between only two states, so the third one can be ignored. In **Fig. 3.3** a comparison between time of evolution of $\langle \sigma_x \rangle$ under the action of these two interaction Hamiltonians is shown

$$H_1 = \frac{\delta(t)}{2}\sigma_z + \frac{\Omega}{2}\sigma_x \tag{3.15}$$

$$H_2 = \frac{\delta(t)}{2}. \tag{3.16}$$

We consider $|+\rangle_x = \frac{1}{\sqrt{2}}(|0\rangle + |1\rangle)$ as the initial state.

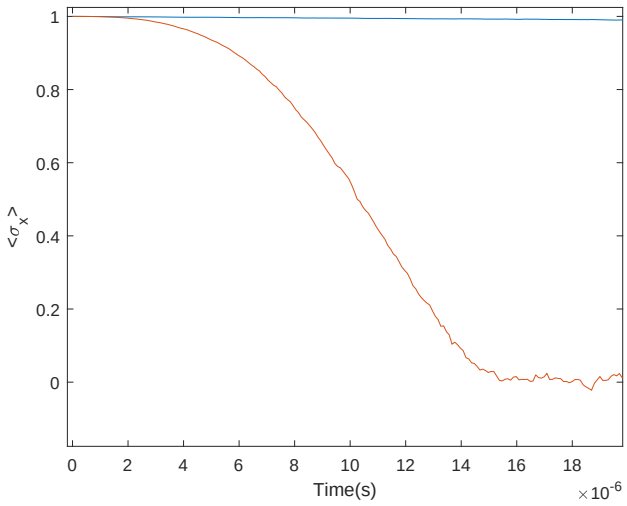

Figure 3.3: $\langle\sigma_x\rangle$ with respect to time (seconds). For this simulation same numerical values as in figure 3.2 have been used. Apart from that we have considered $\tau = 1$ ms as correlation time and $T_2^* = 10$ μs in order to characterize the noise in our system[**6**]. We averaged 1500 shots. We used 65.450 s to simulate this.

As we can see the Hamiltonian that has the term of the driving in it, maintains the initial state $|+\rangle_x = \frac{1}{\sqrt{2}}(|1\rangle + |0\rangle)$, for a much longer time. Namely, introducing the driving field we are able to extend the coherence time of the system. This way we will be able to take advantage of the quantum properties of the NV Centre and use it to apply a protocol to perform NNMR.

3.2 Sensing of ^{13}C nucleus

Finally, we are going to describe the protocol used to detect a carbon atom in the surroundings of the NV centre. This protocol basically aims to achieve the Hartmann-Hahn condition. Once we cover this issue we will perform a simulation of the detection of a ^{13}C nucleus close to the impurity.

3.2.1 Interaction between NV-Centre and ^{13}C nucleus

The Hamiltonian of a system consisting of a NV Centre and a ^{13}C nucleus under the action of magnetic file ($\vec{B} = B_z\hat{z}$) is

$$H = D_{gs}\mathrm{S}_z^2 - \gamma_e B_z \mathrm{S}_z - \gamma_{^{13}\mathrm{C}} B_z \mathrm{I}_z \tag{3.17}$$

S_z represents the z-spin operator of the NV Centre while I_z represents the z-spin operator of the ^{13}C nucleus. These two operators act on different Hilbert spaces. For the sake of simplicity we still take $\hbar = 1$, that is, we will consider these operators as Pauli matrices acting on different spaces. The one acting on the space of the NV centre is a 3×3 Pauli Matrix because $\mathrm{S} = 1$ and the one acting on the space of the nucleus i a 2×2 Pauli Matrix because $\mathrm{I} = 1/2$. $\gamma_e = 2\pi \times 28$ GHz/T and $\gamma_{^{13}\mathrm{C}} = 2\pi \times 10$ MHz/T are the gyromagnetic ratios of the NV Centre and the ^{13}C nucleus respectively.

We should add the magnetic dipole-dipole interaction term

$$H_{dd} = \frac{1}{r^3}\left[\vec{\mathrm{S}} \cdot \vec{\mathrm{I}} - (\vec{\mathrm{S}} \cdot \hat{n})(\vec{\mathrm{I}} \cdot \hat{n})\right] \tag{3.18}$$

If we calculate the interaction picture with respect to $D_{gs}\mathrm{S}_z^2 - \gamma_e B_z \mathrm{S}_z$ the terms that include S_x and S_y rotate much faster that D_{gs}. Thus if we apply the RWA, we can rewrite H_{dd} simply as

$$S_z(\vec{\mathrm{A}} \cdot \vec{\mathrm{I}}) \tag{3.19}$$

where

$$\vec{\mathrm{A}} = \frac{\mu_0 \gamma_{^{13}\mathrm{C}} \gamma_e}{2r^3}\left[\hat{z} - \frac{3(\hat{z} \cdot \vec{r})\vec{r}}{|\vec{r}|^2}\right] \tag{3.20}$$

Where $\mu_0 = 4\pi \cdot 10^{-7} NA^{-2}$ is the vacuum magnetic permeability. The actual formula would have an additional $\hbar^2$ term multiplying, but we took $\hbar = 1$. Nevertheless, when performing the simulation we need to multiply a $\hbar$ term for $\vec{A}$ to preserve the scale.

We also introduce the driving field to extend the coherence time and to cause Rabi cycles.

$$\Omega\sigma_x \cos(\omega t). \tag{3.21}$$

We explained above that in order to allow transitions between the $|0\rangle$ state of the NV Centre and one of the $|\pm 1\rangle$ states, $\omega = D_{gs} \pm \gamma_e B_z$. Besides, in the interaction picture with respect to $D_{gs}\mathrm{S}_z^2 - \gamma_e B_z \mathrm{S}_z$ we can ignore all the terms

that oscillate much faster or much slower than $D_{gs} \pm \gamma_e B_z$. So if we write the complete interaction Hamiltonian we get the following

$$H_{dd}^I = -\gamma_{^{13}\mathrm{C}} B_z \mathrm{I}_z + \mathrm{S}_z(\vec{\mathrm{A}} \cdot \vec{\mathrm{I}}) + \frac{\Omega}{2}\sigma_x. \tag{3.22}$$

As stated above S_z is a 3×3 matrix, but we are going to consider only the transition between two levels. We can manipulate S_z so it only takes into account the transition between $|0\rangle$ and $|1\rangle$ levels. This way we will get a 2×2 matrix instead of a 3×3 this we will allow for a more efficient computation when performing the simulation.

$$S_z = -|-1\rangle\langle -1| + |1\rangle\langle 1| = \frac{|1\rangle\langle 1| + |0\rangle\langle 0| - |0\rangle\langle 0| + |1\rangle\langle 1|}{2} - |-1\rangle\langle -1| \tag{3.23}$$

The last term can be ignored in the interaction picture because, as we showed earlier, when we apply an external oscillating field that has the same oscillating frequency as the splitting between levels $|0\rangle$ and $|1\rangle$ there are only transitions between this states. This way we get,

$$H_{dd}^I = -\gamma_{^{13}\mathrm{C}} B_z \mathrm{I}_z + \frac{1}{2}(\mathbb{1} + \sigma_z)\,\vec{\mathrm{A}} \cdot \vec{\mathrm{I}} + \frac{\Omega}{2}\sigma_x. \tag{3.24}$$

We can rewrite this as follows

$$H_{dd}^I = \left(\frac{\mathrm{A}_1\mathrm{I}_x + \mathrm{A}_2\mathrm{I}_y + \mathrm{A}_3\mathrm{I}_z}{2} - \gamma_{^{13}\mathrm{C}} B_z \mathrm{I}_z\right) + \frac{\sigma_z}{2}\vec{\mathrm{A}} \cdot \vec{\mathrm{I}} + \frac{\Omega}{2}\sigma_x. \tag{3.25}$$

Finally,

$$H_{dd}^I = -w\hat{w} \cdot \vec{\mathrm{I}} + \frac{\sigma_z}{2}\vec{\mathrm{A}} \cdot \vec{\mathrm{I}} + \frac{\sigma_x \Omega}{2} \tag{3.26}$$

Hartmann-Hahn condition

If we took the interaction Hamiltonian with respect to $H_0 = -w\hat{w} \cdot \vec{\mathrm{I}} + \dfrac{\sigma_x \Omega}{2}$ we would get

$$H_{eff} = e^{iH_0 t}\frac{\sigma_z \vec{\mathrm{A}} \cdot \vec{\mathrm{I}}}{2}e^{-iH_0 t} = e^{(i\frac{\Omega}{2}\sigma_x t)}\frac{\sigma_z}{2}e^{(-i\frac{\Omega}{2}\sigma_x t)}e^{(-iw\hat{w}\cdot\vec{\mathrm{I}}t)}\vec{\mathrm{A}} \cdot \vec{\mathrm{I}}e^{(iw\hat{w}\cdot\vec{I}t)}. \tag{3.27}$$

If we use the relation $e^{i\vec{I}\hat{l}\phi}\vec{I}\vec{b}e^{-i\vec{I}\hat{l}\phi} = \vec{I}\left[(\vec{b} - (\vec{b}\cdot\hat{l})\hat{l})\cos\phi - \hat{l} \times \vec{b}\sin\phi + (\vec{b}\cdot\hat{l})\hat{l}\right]$ we get

$$H_{eff} = \frac{1}{2}\left(e^{(i\frac{\Omega}{2}t)}\left|1\right\rangle\left\langle 0\right| + e^{(-i\frac{\Omega}{2}t)}\left|0\right\rangle\left\langle 1\right|\right)\left(\mathrm{A}_x^{\perp}\mathrm{I}_x\cos(wt) + \mathrm{A}_y^{\perp}\sin(wt) + \mathrm{A}_z^{\parallel}\mathrm{I}_z\right) \tag{3.28}$$

where $\mathrm{A}_x^{\perp} = |\vec{\mathrm{A}} - (\vec{\mathrm{A}}\cdot\hat{w})\hat{w}|$, $\mathrm{A}_y^{\perp} = |\hat{w}\times\vec{\mathrm{A}}|$ and $\mathrm{A}_z^{\parallel} = |(\vec{\mathrm{A}}\cdot\hat{w})\hat{w}|$.

If we now take $w = \Omega/2$ and apply the RWA, we get

$$H_{eff} = \frac{\mathrm{A}_x^{\perp}}{2}\left[\left|1\right\rangle\left\langle 0\right| I^{+} + \left|0\right\rangle\left\langle 1\right| I^{-}\right] \tag{3.29}$$

with $\mathrm{I}^{\pm} = \frac{1}{2}\left(\mathrm{I}_x \pm i\mathrm{I}_y\right)$.

This result indicates that the NV centre only transitions between levels when $\Omega = 2w$. This is the so called Hartmann-Hahn condition [**10**].

Knowing this we can sense a surrounding nucleus. We can increase the B_x field to change Ω. Once $2w = \Omega$ the NV centre would start flipping between levels and the spin state would also change. Taking note of the field B_x where this happens we could deduce the kind of nucleus we are detecting.

3.3 Numerical simulations

3.3.1 Noiseless simulation

First we simply simulated (**Eq. 3.26**) for different Ω to check that what we predicted is true. To simulate the quantum system we began in the state $(\left|\psi\right\rangle\left\langle\psi\right|)\otimes\rho_I$. Where ρ_I indicates a random state of the 13-Carbon nucleus. We represent that with a density matrix,

$$\rho_I = \frac{1}{2}\begin{bmatrix}1 & 0\\ 0 & 1\end{bmatrix}. \tag{3.30}$$

The initial state of the NV centre is represented by a density matrix too. Taking $\left|\psi\right\rangle = \frac{1}{\sqrt{2}}\left(\left|0\right\rangle + \left|1\right\rangle\right)$ we get,

$$\rho_0 = \frac{1}{2}\begin{bmatrix}1 & 1\\ 1 & 1\end{bmatrix}. \tag{3.31}$$

The initial state is consequently represented by the Kronecker product of these two matrices.

We fix the position of the nucleus and the B_z field. This way the w frequency is also fixed. Then we let the system evolve under the action of (**3.26**) for different Ω. To check the change in the state of the NV Centre we calculate $\langle\sigma_x\rangle$ after some time. In **Fig. 3.4** we present the results of the simulation.

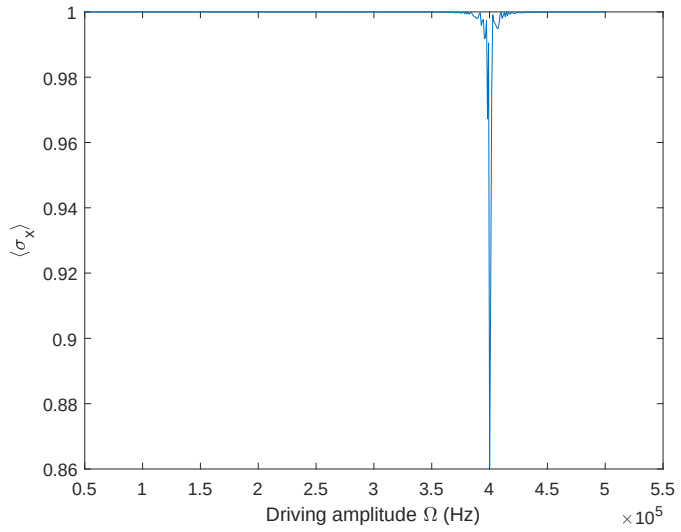

Figure 3.4: $\langle\sigma_x\rangle$ for different Ω frequencies (Hz). The parameters set were $\vec{r} = (2, 1, 3) \cdot 10^{-9}$m (position of the 13-Carbon atom), $B_z = 0.02$T and $w = 2.00 \cdot 10^5$ Hz. We let the system evolve for times $t = 5000/\Omega$ and for 500 different frequencies between $5.02 \cdot 10^4$ Hz and $5.00 \cdot 10^5$ Hz. We needed 7.911 s to compute this.

As expected we got a peak, that is, a change in the state of the NV centre when we made the simulation with $2w = \Omega = 4.00 \cdot 10^5$Hz.

3.3.2 Simulation with noise

In a real situation we would be forced to repeat the experiment several times in order to get accurate information. We should average the results obtained in different 'shots' so we could distinguish the noise introduced by the spin bath and the measuring instruments from the actual changes in the state of the NV centre. The stochastic function about which we have widely spoken helps us to depict such scenario. The Hamiltonian we will simulate is

$$H_{dd}^I = -w\hat{w} \cdot \vec{\mathrm{I}} + \frac{\sigma_z}{2}\vec{\mathrm{A}} \cdot \vec{\mathrm{I}} + \frac{\sigma_x \Omega}{2} + \frac{\delta(t)}{2}\sigma_z \tag{3.32}$$

where $\delta(t)$ is the Ornstein-Uhlenbeck process.

First, we tried to carry out the simulation with the same magnetic field as in the noiseless case. We got **Fig. 3.5**.

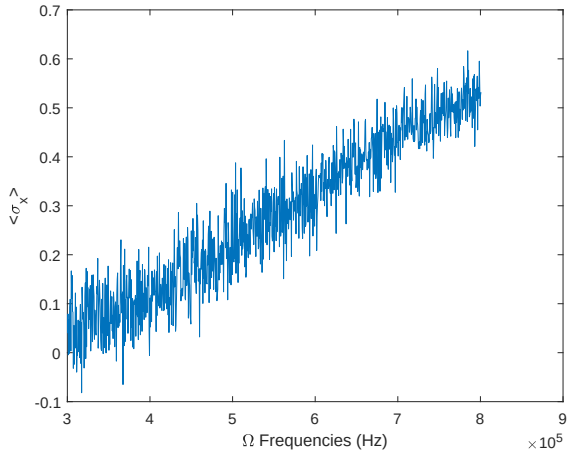

Figure 3.5: $\langle \sigma_x \rangle$ with respect to Ω frequencies with $B_z = 0.02$T. In this simulation we took $T_2^* = 10$ μs and $\tau = 1$ ms to characterise our noise. We let the system evolve for a time $t = 100/\Omega$ and for 1000 different Ω. We repeated the evolution 100 times and averaged the result. The time needed to carry our this simulation was 3366.452 s.

We cannot see a change in the state. This is probably due to the frequencies w and Ω lying close to the central frequency of the Ornstein-Uhlenbeck process. Namely, the noise is destroying our simulation. To avoid this we must get a greater w and Ω so it lies away from that central frequencies. To accomplish this we simply apply a greater B_z and B_x fields. By doing so we get the **Fig. 3.6**

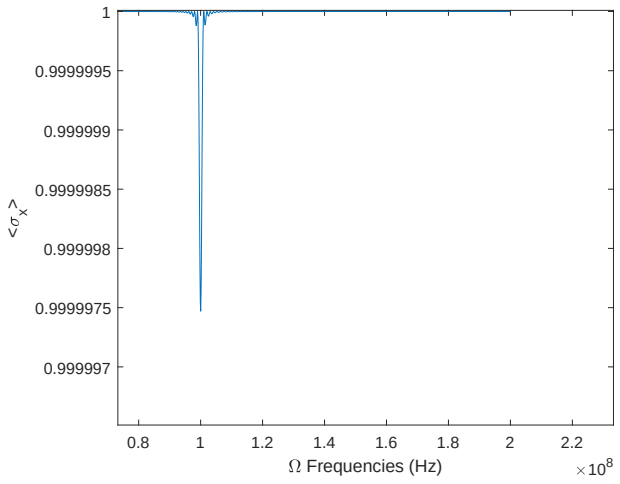

Figure 3.6: $\langle \sigma_x \rangle$ with respect to Ω frequencies with $B_z = 5$T. In this simulation we took $T_2^* = 10$ μs and $\tau = 1$ ms to characterise our noise. We let the system evolve for a time $t = 100/\Omega$ and for 1000 different Ω. We repeated the evolution 100 times and averaged the results.$w = 0.5 \times 10^8$ Hz. $\vec{r} = (2, 1, 3) \cdot 10^{-9}$ m. The time to compute this was 3305.561 s.

As we can see there is a peak in precisely where $2w = \Omega$. This would in a

real experiment confirm the existence of a nucleus nearby. By noting at which frequency the flipping occurs we could deduce the nucleus' gyromagnetic ratio (which was known for us during the simulation) and deduce exactly what kind of nucleus we are detecting.

However, in the simulation we carried out the scale of the peak is distinguishable only because MATLAB enables us to have such precession. In a real experiment such peak would probably be impossible to detect. We should simulate the evolution of the system for a longer time in order to have a better scale, that is, to have a deeper peak. We did not simulate the evolution of the system for a longer time because the computation time would increase a lot.

Conclusions

Throughout this work we have revised some of the most important characteristics, properties and applications of the NV Centre. We then have presented the most important mathematical tools needed to simulate and apply a protocol to perform Nanoscale Nuclear Magnetic Resonance.

The results predict a change on the the state of the NV centre when we introduce a driving field whose amplitude is equal to the double of w and whose frequency is equal to the splitting between $|0\rangle$ and $|1\rangle$ levels. This protocol could be used in an actual experiment to detect not only one but several quantum entities both ^{13}C nuclei or other. It all comes down to calculating the Larmor frequency and deducing which nuclei it belongs to. If we had several nuclei surrounding our NV centre we would get similar peaks as the one in **Fig. 3.6** but for different Ω frequencies depending on their position and gyromagnetic ratio.

Nevertheless, we were restricted to simulating the sensing of just one nucleus because of the computation time. Making the last simulation took 3305.561 seconds. Each extra nuclei added to the simulation would have increased the computation time exponentially. Therefore, to make more accurate predictions and to simulate more complex scenarios we are forced to use a more powerful computer.

Thus, we can conclude that the application of the kind of protocol described here can be used to effectively sense surrounding atoms. Further development of this kind of protocols could for example result, as mentioned, in a way to know the exact 3D structure of proteins and molecules. This structure is one of the factors that determines the behaviour and properties molecules have. Thus, deepening in this issue could let us reach a great milestone in science.

Bibliography

[1] *https://www.britannica.com/science/color-center*

[2] Jahnke, K.D. *Coherent control of single spins in diamond*: pages 1-19. 2012.

[3] Doherty, M.W., Manson, N.B., Delaney, P., Jelezko, F., Wachtrup, J. and Hollenberg, L.C.L. *The nitrogen-vacancy colour centre in diamond.* 2013.

[4] Hopper, D.A., Shulevitz, H.J. and Bassett, L.C.*Spin Readout Techniques of the Nitrogen-Vacancy Center in Diamond*: pages 6-8. 2018.

[5] Robledo, L., Childress, L., Hannes, B., Hensen, B., Alkemade P.F.A., Hanson, R. *High-fidelity projective readout of a solid-state spin quantum register.* 2011.

[6] *Private communication with Prof. Boris Naydenov (Ulm University, Germany)*

[7] Schirhgal, R., Chang K., Loretz, M. and Degen, C.L.*Nitrogen-Vacancy Centers in Diamond: Nanoscale sensors for Physics and Biology.* 2013.

[8] Sakurai, J.J.*Modern quantum mechanics.* 1994.

[9] Puebla, R., Casanova,J. and Plenio, M. *A robust scheme for the implementation of the quantum Rabi model in trapped ions*: pages 2-8. 2017.

[10] Hartmann, S.R. and Hahn, E.L.*Nuclear Double Resonance in the Rotating Frame.* 1962.